

Effects of Adhesive Characteristics between Matrix and Reinforced Nanoparticle of AA6063/Carbon Black Nanocomposites

T. Prasad¹, A. C. Reddy²

¹Ph.D (Mechanical Engineering), JNTU University, Hyderabad, India

²Professor, BOS-Chairman, Department of Mechanical Engineering, JNT University, Hyderabad-500 085, India

Abstract: In this paper the effects of adhesive characteristics between the matrix and the reinforced nanoparticle of AA6063/carbon black nanocomposites were analyzed through RVE models using finite element analysis software. The adhesive bond was broken between the carbon black nanoparticle and AA6063 alloy matrix in the nanocomposite when the stress was exceeded the tensile strength of the matrix. The RVE was expanded elastically away from the nanoparticle in the direction of the tensile loading. The presence voids could reduce the strength and stiffness of the nanocomposite.

Keywords: AA6063, carbon black, RVE model, nanocomposite, finite element analysis.

1. Introduction

The superior stiffness of ceramic particles can escort to the incremental raise of a composite's stiffness [1, 2]. Micron-sized particles cause a decrease in the impact resistance. On the other hand, using nanoparticles can lead to better impact and wear performance [3]. The existence of an interphase region with a higher strength and modulus than the matrix material is the source for the composites to have superior mechanical properties [4]. Interfacial debonding can cause shear yielding of the matrix around the particles. Very small particles are difficult to disperse, creating agglomerates that behave as a large, single particle [5, 6]. The tensile properties of nanocomposites, including their tensile strength and elastic modulus, have been analyzed via micromechanical models. The modulus magnitude depends on the interfacial adhesion and the matrix's crystalline structure [7].

The strength of a particulate metal matrix composite depends on the strength of the weakest zone and metallurgical phenomena in it [8]. Considering adhesion, formation of precipitates, particle size, agglomeration, voids/porosity, obstacles to the dislocation, and the interfacial reaction of the particle/matrix, the formula [9] for the strength of composite is stated below:

$$\sigma_c = \left[\sigma_m \left\{ \frac{1-(v_p+v_v)^{2/3}}{1-1.5(v_p+v_v)} \right\} \right] e^{m_p(v_p+v_v)} + k d_p^{-1/2} \quad (1)$$

where, $k = E_m m_m / E_p m_p$; v_v and v_p are the volume fractions of voids/porosity and nanoparticles in the composite respectively, m_p and m_m are the poisson's ratios of the nanoparticles and matrix respectively, d_p is the mean nanoparticle size (diameter) and E_m and E_p is elastic moduli of the matrix and the particle respectively.

The elastic modulus is a measure of the stiffness of a material and is a quantity used to characterize materials. Elastic modulus is the same in all orientations for isotropic materials. Anisotropy can be seen in many composites. The

equation [9] to find Young's modulus including the effect of voids/porosity in the composite is given below:

$$\frac{E_c}{E_m} = \left(\frac{1-v_v^{2/3}}{1-v_v^{2/3}+v_v} \right) + \frac{1+(\delta-1)v_p^{2/3}}{1+(\delta-1)(v_p^{2/3}-v_p)} \quad (2)$$

where, $\delta = E_p/E_m$. E_c , E_m and E_p are the elastic moduli of composite, matrix and nanoparticles respectively.

The finite element procedure and analytical methods have been exceptionally effective in determining the mechanical properties of non-homogeneous materials like composites [10]. In finite element numerical models very fine meshes need to be applied inside and around the interphase layers which results in large number of degrees of freedom. Currently, the use of a representative volume element (RVE) or a unit cell [11] of the composite microstructure, in conjunction with a finite element (FE) analysis tool is well established for examining the effective material properties and understanding the micromechanics of the composite materials.

AA6063 is an aluminum alloy with magnesium and silicon as the alloying elements. AA6063 is used in extruded shapes for architecture such as window frames, door frames, roofs and sign frames. Carbon black is a material with high economic importance containing pure carbon. It is used in many products including car tires, printer toner, dyes for leather or textiles and mascara.

The objective the present paper was to investigate the effects of adhesive characteristics between the matrix and the reinforced nanoparticle of AA6063/carbon black nanocomposites through RVE models using finite element analysis software.

2. Materials and Methods

The matrix material was AA6063 aluminum alloy. The reinforcement material was carbon nanoparticles of average size 100nm. The morphology of carbon nanoparticles was spherical, and they appear as a black powder (figure 1).

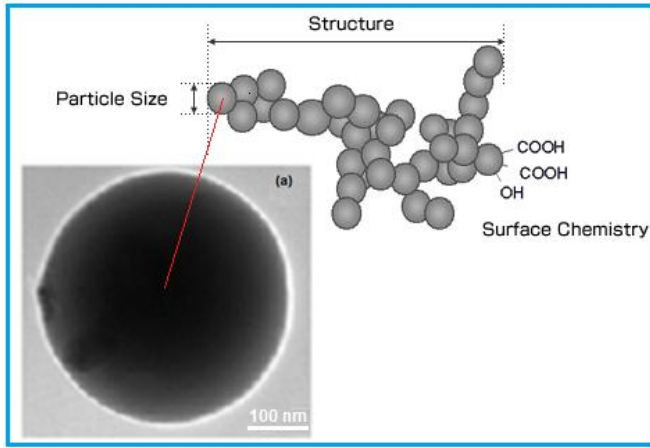


Figure 1: Morphology of carbon black nanoparticle.

2.1 Preparation of composite specimens

The matrix alloys and composites were prepared by the stir casting and low-pressure die casting process. The volume fractions of carbon black reinforcement were 10%, 20%, and 30%. AA6063 matrix alloy was melted in a resistance furnace. The crucibles were made of graphite. The melting losses of the alloy constituents were taken into account while preparing the charge. The charge was fluxed with coverall to prevent dressing. The molten alloy was degasified by tetrachlorethane (in solid form). The crucible was taken away from the furnace and treated with sodium modifier. Then the liquid melt was allowed to cool down just below the liquidus temperature to get the melt semi solid state. At this stage, the preheated (500°C for 1 hour) reinforcement particles were added to the liquid melt. The molten alloy and reinforcement particles are thoroughly stirred manually for 15 minutes. After manual steering, the semi-solid, liquid melt was reheated, to a full liquid state in the resistance furnace followed by an automatic mechanical stirring using a mixer to make the melt homogenous for about 10 minutes at 200 rpm. The temperature of melted metal was measured using a dip type thermocouple. The preheated cast iron die was filled with dross-removed melt by the compressed (3.0 bar) argon gas [9]. The as-cast microstructure of AA6063/carbon black is shown in figure 2. The round-black particles are carbon particles in the microstructure.

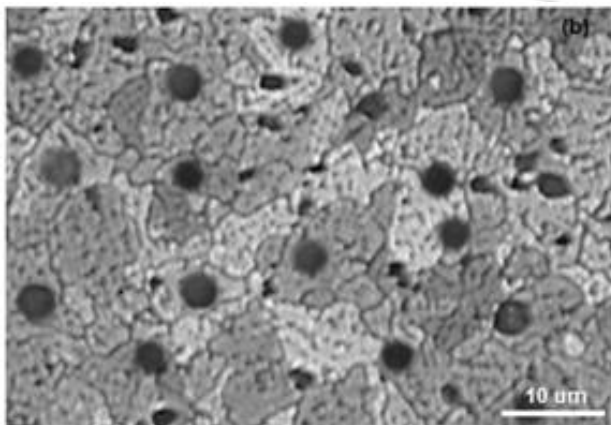


Figure 2: Microstructure of as-cast AA6063/carbon black nanocomposite.

2.2 Heat treatment

Prior to the machining of composite samples, a solution treatment was applied at 500°C for 1 hour, followed by quenching in cold water. The samples were then naturally aged at room temperature for 100 hours.

2.3 Tensile tests

The heat-treated samples were machined to get flat-rectangular specimens (figure 3) for the tensile tests. The tensile specimens were placed in the grips of a Universal Test Machine (UTM) at a specified grip separation and pulled until failure. The test speed was 2 mm/min (as for ASTM D3039). A strain gauge was used to determine elongation as shown in figure 3.

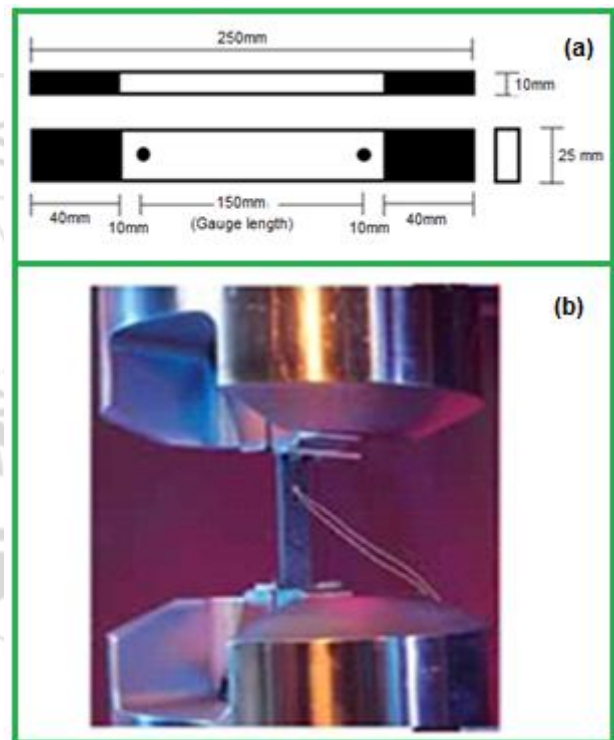


Figure 3: Shape and dimensions of tensile specimen; (b) tensile testing.

2.4 Optical and SEM analysis

An image analyzer was used to study the distribution of the reinforcement particles within the AA6063 aluminum alloy matrix. The polished specimens were ringed with distilled water, and etched with 0.5% HF solution for optical microscopic analysis. Fracture surfaces of the deformed/fractured test samples were analyzed with a scanning electron microscope (SEM) to define the macroscopic fracture mode and to establish the microscopic mechanisms governing fracture. Samples for SEM observation were obtained from the tested specimens by sectioning parallel to the fracture surface and the scanning was carried using S-3000N Toshiba SEM.

2.5 RVE modeling using finite element analysis (FEA)

The representative volume element (RVE or the unit cell) is the smallest volume over which a measurement can be made

that will yield a value representative of the whole. In this research, a cubical RVE was implemented to analyze the tensile behavior AA6063/carbon black nanocomposites (figure 4). The determination of the RVE's dimensional conditions requires the establishment of a volumetric fraction of spherical nanoparticles in the composite. Hence, the weight fractions of the particles were converted to volume fractions. The volume fraction of a particle in the RVE V_p (RVE) is determined using equation:

$$v_p(\text{RVE}) = \frac{\text{Volume of nanoparticle}}{\text{Volume of RVE}} = \frac{16}{3} \times \left(\frac{r}{a}\right)^3 \quad (3)$$

where, r represents the nanoparticle radius and a indicates the length of the cubical RVE. The volume fraction of the nanoparticles in the composite (v_p) was chosen to be 0.10, 0.20 and 0.30; the nanoparticle radius (r) was taken to be 100 nm.

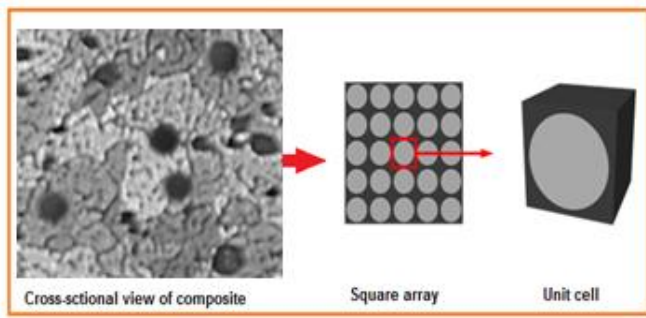


Figure 4: The RVE model.

The RVE dimension (a) was determined by equalizing equation (3). The RVE scheme with adhesion (without interphase) was applied between the matrix and the filler. The loading on the RVE was defined as symmetric displacement, which provided equal displacements at both ends of the RVE. To obtain the nanocomposite modulus and yield strength, the force reaction was defined against displacement. The PLANE183 element was used in the matrix and the nanoparticle (table 1). In order to model the adhesion between the matrix and the particle, a COMBIN14 spring-damper element was used. The stiffness of this element was chosen to be unity, which determines the interfacial strength for the interface region. To converge an exact nonlinear solution, it is also important to set the strain rates of the FEM models based on the experimental tensile tests' setups. Hence, FEM models of different RVEs with various particle contents should have comparable error values. In this respect, the ratio of the tensile test speed to the gauge length of the specimens should be equal to the corresponding ratio in the RVE displacement model. Therefore, the rate of displacement in the RVEs was set to be 0.1 (1/min).

Table 1: Elements features, applications and size ranges used in RVE modeling

Element code	Plane 183	Contact 172	Combination 14	Target 169
Feature	Quadrilateral-8 nodes	Linear 3 node	Longitudinal spring-damper	Shape complexity
Application	Matrix and nanoparticle	Interface contact	Elastic modeling of adhesion	Contact bodies

3. Results and Discussion

Figure 5 reveals the optical microstructure of AA6063/carbon black nanocomposites. It was observed that the carbon black nanoparticles were randomly distributed in the AA6063 matrix. Figure 6 describes the tensile strengths of the nanocomposites obtained by FEA, AC Reddy model, and experimental procedure. The tensile strength would increase with an increase of carbon black content in the nanocomposites. The tensile strength (without voids) obtained by the finite element analysis (FEA) were lower than the experimental values. When voids were considered in the composites the interface region was stiffened (with good bonding between particle and matrix) and this caused the tensile strength to remain constant with an increase in the nanoparticles content. This was on account of the failure which was occurred in the regions of voids or in the matrix. The tensile strengths obtained by AC Reddy model (with voids) mentioned Eq. (1) and experimental results were almost equal.

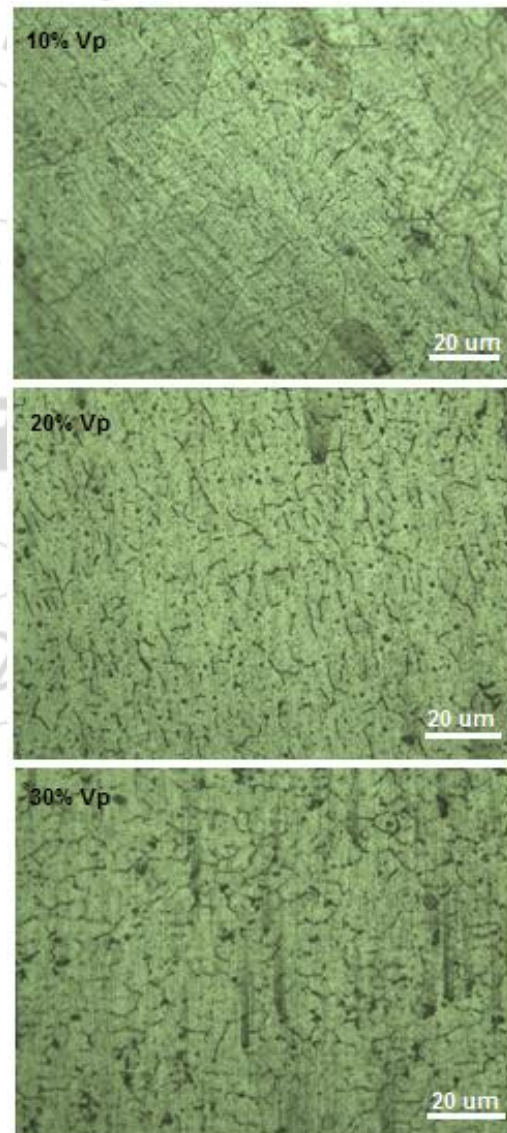


Figure 5: Optical microstructures of AA6063/carbon black nanocomposites.

The adhesive bond was broken between the carbon black nanoparticle and AA6063 alloy matrix in the nanocomposite

when the stress was exceeded the ultimate tensile strength (241 MPa) of the matrix as shown in figure 7. The region of red color is the failure zone between the nanoparticle and the matrix. It is also observed from figure 7 that the load transfer from the matrix to the nanoparticle has increased with increasing content of carbon black nanoparticles in the composite.

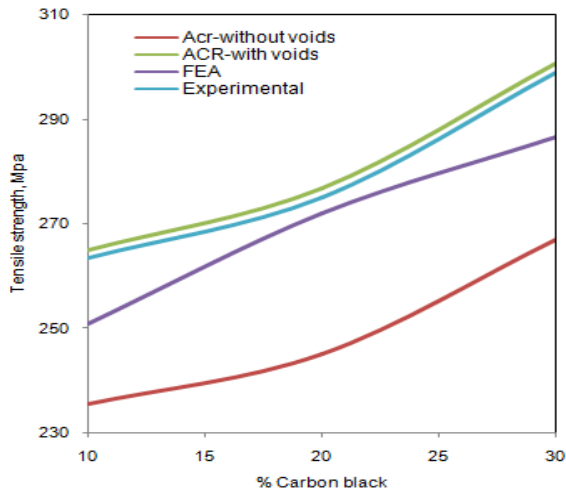


Figure 6: Effect of volume fraction on tensile strength.

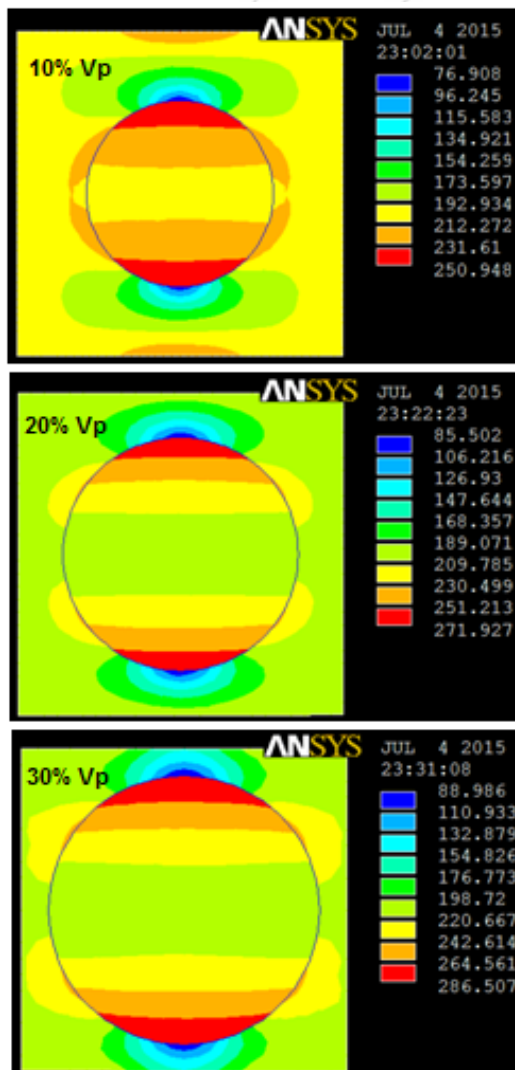


Figure 7: Tensile stress along the tensile loading.

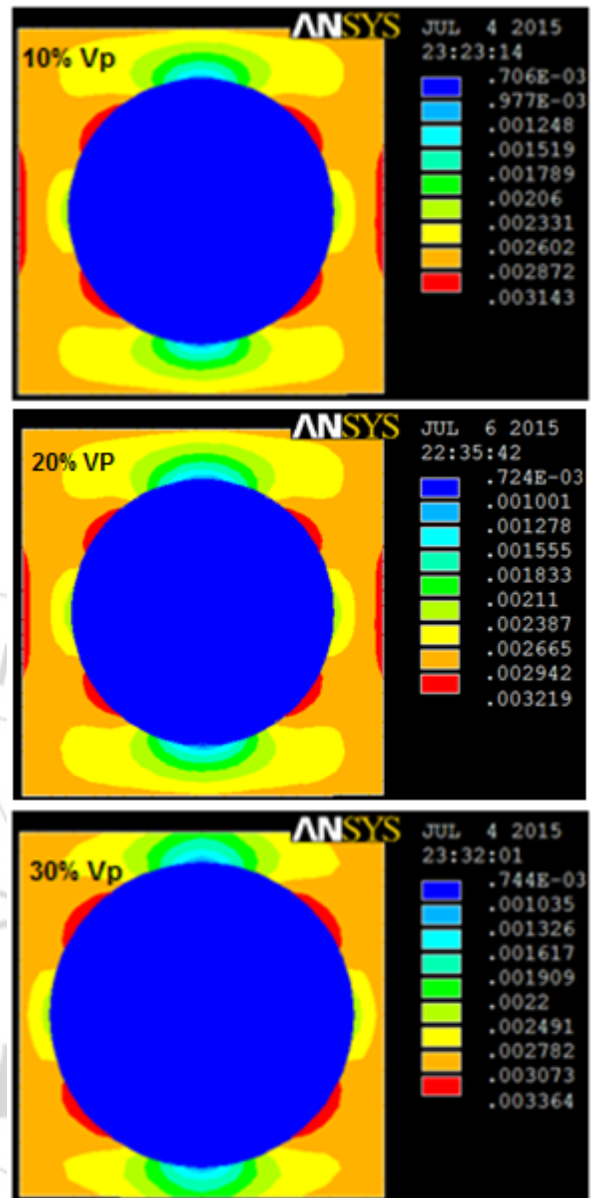


Figure 8: Elastic strain in the direction of tensile loading.

Figure 8 illustrates the elastic strain contours of the RVE models. According to figure 8, the RVE was expanded elastically away from the nanoparticle in the direction of the tensile loading. This could increase the contact area between the particle and the matrix in the perpendicular direction to the tensile loading and decreases the contact area between the particle and the matrix in the direction of the tensile loading. In addition, the deformation was propagated in the normal direction to the tensile loading.

Figure 9 shows the variations of von Mises stress in the nanocomposites. The von Mises stress had increased with an increase of carbon black content. It was observed that the interfacial debonding was high between the particle and the matrix because the local stress concentration around the nanoparticle increases with an increase in the volume fraction of carbon black in the nanocomposite.

Table 2 gives the elastic (tensile) moduli of the nanocomposites obtained by the Rule of Mixtures, FEA and AC Reddy model with respect to the volume fraction of carbon black nanoparticles. By increasing the nanoparticles

the elastic modulus had increased appreciably. AC Reddy model as mentioned in Eq. (2) considers the influence of voids/porosity in the nanocomposite. The values obtained by this model are lower than those obtained from FEA because the voids are not considered in the finite element analysis of the nanocomposites. This is due to the fact that the existence of voids in the nanocomposites. The presence of voids, even at a very low volume fraction, can significantly degrade the material properties [12].

RVE has expanded elastically away from the nanoparticle in the direction of the tensile loading. By increasing the nanoparticles the elastic modulus has increased appreciably. The presence voids can reduce the strength and stiffness of the nanocomposite.

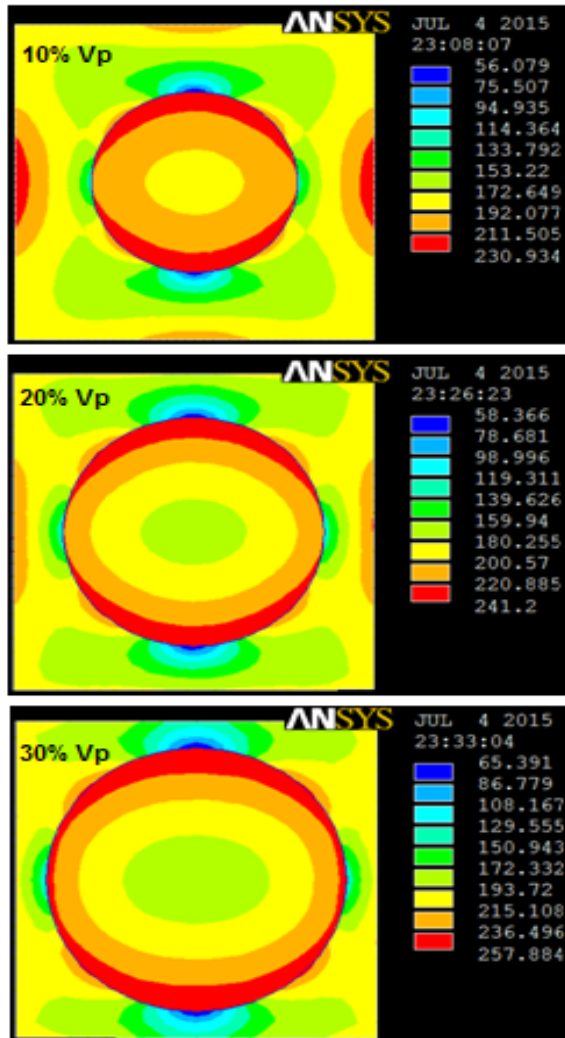


Figure 9: von Mises stress.

Table 2: Elastic modulus AA6063/carbon black nanocomposite

Model	Elastic Modulus, GPa		
	10% Vp	20% Vp	30% Vp
Rule of Mixture	88.05	93.36	98.68
AC Reddy	148.33	158.54	167.15
FEA	165.21	174.87	177.18

4. Conclusion

The tensile strength is increased with an increase of carbon black content in the nanocomposites. The adhesive bond is broken between the carbon black nanoparticle and AA6063 alloy matrix in the nanocomposite when the stress is exceeded the tensile strength (241 MPa) of the matrix. The

References

- [1] A.Chennakesava Reddy, "Mechanical properties and fracture behavior of 6061/SiCp Metal Matrix Composites Fabricated by Low Pressure Die Casting Process," Journal of Manufacturing Technology Research, vol.1, no. 3/4, pp. 273-286, 2009.
- [2] A. Chennakesava Reddy, Essa Zitoun, Tensile behavior of 6063/Al₂O₃ particulate metal matrix composites fabricated by investment casting process, "International Journal of Applied Engineering Research, vol.1, no.3, pp. 542-552, 2010.
- [3] K. Friedrich, Z. Zhang , A.K. Schlarb, "Effects of various fillers on the sliding wear of polymer composites," Composites Science and Technology, vol. 65, pp.2329-2343, 2005.
- [4] M. Romanowicz, "Progressive failure analysis of unidirectional fiber-reinforced polymers with inhomogeneous interphase and randomly distributed fibers under transverse tensile loading," Composites part A, vol. 41, pp.1829-1838, 2010.
- [5] Y.S.Thio, A.S.Argon, R.E.Cohen, M.Weinberg, "Toughening of Isotactic Polypropylene with CaCO₃ Particles," Polymer, vol. 43, pp. 3661-3674, 2002.
- [6] A. Chennakesava Reddy, "Tensile fracture behaviour of 7072/SiCp metal matrix composites fabricated by gravity die casting process," Materials Technology: Advanced Performance Materials, vol.26, no.5, pp..257-262, 2011.
- [7] K. Wang, J. Wu, L. Ye, H. Zeng, "Mechanical properties and toughening mechanisms of polypropylene/barium sulfate composites," Composites: Part A, vol. 34, pp.1199-1205, 2003.
- [8] A. Chennakesava Reddy, B. Kotiveerachari, "Influence of microstructural changes caused by ageing on wear behavior of Al6061/SiC composites," Journal of Metallurgy & Materials Science, vol.53, no.1, pp. 31-39, 2011.
- [9] A. Chennakesava Reddy, "Influence of Particle Size, Precipitates, Particle Cracking, Porosity and Clustering of Particles on Tensile Strength of 6061/SiCp Metal Matrix Composites and Validation Using FEA," International Journal of Material Sciences and Manufacturing Engineering, vol.42, no.1, pp. 1176-1186, 2015.
- [10] A. Chennakesava Reddy, "Strengthening mechanisms and fracture behavior of 7072Al/Al₂O₃ metal matrix composites," International Journal of Engineering Science and Technology, vol.3, no.1, pp.6090-6100, 2011.
- [11] R. Hill, "Elastic properties of reinforced solids: some theoretical principles," Journal of the Mechanics and Physics of Solids, vol. 11, no.5, 1963.
- [12] N.C.W. Judd, W.W. Wright, "Voids and their effects on the mechanical properties of composites – an appraisal", SAMPE Journal, vol.14, no.1, pp.10-14, 1978.